Engineering Curvature-Induced Anisotropy in Thin Ferromagnetic Films

Oleg A. Tretiakov*
Institute for Materials Research, Tohoku University, Sendai 980-8577, Japan and School of Natural Sciences, Far Eastern Federal University, Vladivostok 690950, Russia

Massimiliano Morini
Dipartimento di Scienze Matematiche Fisiche e Informatiche, Università di Parma, Parma 43124, Italy

Sergiy Vasylkevych and Valeriy Slastikov
School of Mathematics, University of Bristol, Bristol, BS8 1TW, United Kingdom

(Received 26 October 2016; revised manuscript received 17 July 2017; published 17 August 2017)

We investigate the effect of large curvature and dipolar energy in thin ferromagnetic films with periodically modulated top and bottom surfaces on magnetization behavior. We predict that the dipolar interaction and surface curvature can produce perpendicular anisotropy which can be controlled by engineering special types of periodic surface structures. Similar effects can be achieved by a significant surface roughness in the film. We demonstrate that, in general, the anisotropy can point in an arbitrary direction depending on the surface curvature. Furthermore, we provide simple examples of these periodic surface structures to show how to engineer particular anisotropies in thin films.

DOI: 10.1103/PhysRevLett.119.077203

The puzzle of perpendicular magnetic anisotropy (PMA) origin in thin ferromagnetic films has a long history, dating back to Néel, who was the first to address it [1]. Later, there have been several other attempts in this direction [2–7]. In particular, in multilayers consisting of alternating ferromagnetic and heavy-metal (such as Pt) layers, PMA has been attributed to strong spin-orbit interaction at the interfaces [8–13]. However, in thin magnetic films, PMA may exist [14,15] without an additional heavy-metal layer, which enhances spin-orbit interaction in the system, thus pointing to a more general perpendicular anisotropy mechanism.

Previous studies of magnetic nanostructures with large-scale smoothly varying curvature have shown that the magnetization prefers to stay in a plane tangential to the surface [7,16–21]. This general principle applies when the surface variations occur on a scale larger than the film thickness (inverse surface curvature is larger than thickness). However, in the case of a rapidly modulated surface, when the inverse curvature is of the same order as the film thickness, the situation might be different, and magnetic anisotropy, dominated by surface curvature effects, may produce preferred directions not tangential to the film surface [5,22]. Nowadays, the film thickness often reaches just a few monolayers, and in this case the surface roughness may lead to these large rapid modulations of geometric curvature and thus be responsible for the PMA in the films.

In this Letter, we aim to understand the effect of large periodic curvature on the shape anisotropy and demonstrate the formation mechanism of perpendicular or any other given direction of magnetic anisotropy by means of the surface engineering of an ultrathin magnetic film. The proposed mechanism does not require any spin-orbit coupling and is related solely to the interplay of surface curvature and dipolar interactions in the film. This possibility may open up a direction to tailor the interfacial magnetic anisotropy in thin ferromagnetic films without any additional layers of heavy metal, which, in turn, may lead to simpler and cheaper ways to engineer systems with any given anisotropy. Nowadays, the curvature effects in thin magnetic films are becoming more accessible due to experimental advances in flexible electronics [23–27], making the proposed method to control the anisotropy experimentally viable in the near future. Moreover, our findings suggest that similar effects might be observed in thin films with significant surface roughness.

The main goal of this Letter is to derive and investigate a comprehensive reduced model of magnetization behavior in thin ferromagnetic films with periodically modulated surfaces; see Fig. 1. We concentrate on the regime where the film thickness is comparable to the amplitude and the period of film surface modulations and derive an effective local two-dimensional (2D) model. Surprisingly, we demonstrate that, in the special case of nearly parallel to each

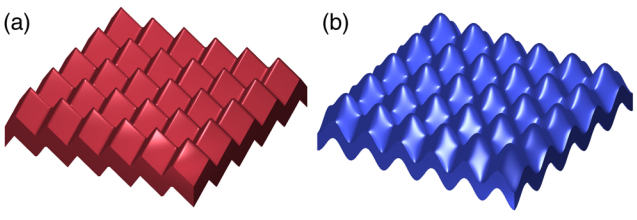

FIG. 1. Examples of engineered periodic magnetic films. (a) The film consisting of pyramids. (b) The film consisting of $\sin^2 x_1 \sin^2 x_2$ shapes.

other surfaces of the film, this extreme geometry is responsible for creating a strong uniaxial shape anisotropy with an arbitrary preferred direction depending on the surface curvature. This rather unexpected outcome suggests that in certain regimes a surface curvature in ultrathin ferromagnetic films may lead to a PMA. Meanwhile, in the cases of a more general curvature, when the top and bottom surfaces are rather different, we show by considering several diverse examples that the magnetization prefers to stay in the film's plane [28].

To tackle the physics of magnetic surfaces with rapid periodic modulations, we employ the method of asymptotic homogenization. Physically, this problem is associated with two scales; the larger one is given by the size of the film's domain where we aim to determine the anisotropy, whereas the smaller one is associated with the period of the film's curvature modulation. The latter scale should be generally much smaller to have a nontrivial effect on anisotropy, which can then be homogenized over the larger film's scale. Formally, the method of asymptotic homogenization proceeds by introducing the fast variable $\mathbf{y} = \mathbf{x}/\varepsilon$ and performing an expansion of unit magnetization $\mathbf{M}$ in small parameter ε:

$$\mathbf{M}_\varepsilon(\mathbf{x}) = \mathbf{M}_0(\mathbf{x}) + \varepsilon \mathbf{M}_1(\mathbf{x}, \mathbf{y}) + O(\varepsilon^2), \tag{1}$$

which generates a hierarchy of problems. The homogenized equation is obtained, and the effective coefficients are determined by solving the so-called "cell problem" for the function $\mathbf{M}_1(\mathbf{x}, \mathbf{x}/\varepsilon)$. For a thin film, small parameter $\varepsilon = t/L$ is physically determined as the ratio of the film thickness t and its typical lateral dimension L (of the order of single domain size).

We study a three-dimensional thin film domain $V_\varepsilon = (\mathbf{x}', x_3)$, where $\mathbf{x}' = (x_1, x_2)$ belongs to the 2D domain ω (the projection of the thin film on the plane) and $\varepsilon f(\mathbf{x}'/\varepsilon) < x_3 < \varepsilon[1 + f(\mathbf{x}'/\varepsilon)]$ with $\varepsilon > 0$ being a constant dimensionless film's thickness. We consider an arbitrary periodic function $f(x_1, x_2)$, which models the film's surface modulation with the periodic cell given by a square of unit length. Typical examples of the surface shape functions that might be considered are $f(\mathbf{x}') = \sin^2(\pi x_1)$, $f(\mathbf{x}') = \sin^2(\pi x_1)\sin^2(\pi x_2)$, or the one shown in Fig. 1(a).

In the standard continuum description, the dimensionless micromagnetic energy containing exchange and dipolar interactions takes the form

$$\mathcal{E}_\varepsilon(\mathbf{M}) = \xi \int_{V_\varepsilon} |\nabla \mathbf{M}|^2 d\mathbf{x} + \int_{\mathbb{R}^3} |\nabla u|^2 d\mathbf{x}, \tag{2}$$

where $\xi = A/(\mu_0 M_s^2 L^2) > 0$ is the dimensionless material parameter, A is the exchange constant, μ_0 is vacuum permeability, M_s is saturation magnetization, and u in the dipolar contribution is determined as the solution satisfying $\Delta u = \mathrm{div}\mathbf{M}$ in the entire space, where magnetization $\mathbf{M}$ is nonzero only within the volume of the film. Because of its nonconvex and nonlocal nature, this variational problem cannot be addressed in its full generality by current analytical methods. However, in the regime of an ultrathin modulated film with the modulation period comparable to its thickness, we are able to reduce the micromagnetic energy (2) to a simpler energy functional, capturing the essence of the magnetization behavior in a sample. This nontrivial task allows us to analytically investigate an effective anisotropy in the film.

To find the validity limits of our model for potential experimental systems, we estimate the range of applicable film thicknesses and lateral dimensions. We require the dimensionless thickness $\varepsilon \ll 1$, and therefore a reasonable estimate of $t/L \sim 0.1$ should provide good applicability of the model. For ultrathin films successfully grown by standard modern techniques, the thickness is roughly $t \sim 1$–10 nm, and therefore the actual sample (domain) dimensions should be $L \sim 100$ nm or larger. Also, for our model to give a good approximation of the full micromagnetic model, the parameter ξ in Eq. (2) should not be much smaller than 1. For realistic experimental values of the exchange constant and saturation magnetization, the length scale $\sqrt{A/(\mu_0 M_s^2)} \sim 30$–$100$ nm, and therefore it falls within the range of applicability of our reduced model.

To study the thin film limit, i.e., the limiting behavior of the energy as $\varepsilon \ll 1$, it is convenient to consider the rescaled energy $E_\varepsilon(\mathbf{m}) = \mathcal{E}_\varepsilon(\mathbf{M})/\varepsilon$ with magnetization $\mathbf{M}(\mathbf{x}', x_3) = \mathbf{m}(\mathbf{x}', x_3/\varepsilon)$. In this case, the main contribution to the energy is coming from the interaction of surface magnetic charges of the largest (top and bottom) surfaces. We note that special care has to be taken, because the magnetization distribution has values on a 2D sphere. Using the ideas of two-scale convergence [29] and Γ-convergence [30], we can find the limiting micromagnetic energy functional as

$$E_0(\mathbf{m}) = \xi \int_\omega h^{\mathrm{ex}}(\nabla \mathbf{m}) d\mathbf{x}' + \int_\omega K^{\mathrm{eff}} \mathbf{m} \cdot \mathbf{m} d\mathbf{x}', \tag{3}$$

where a non-negative convex function h^{ex} vanishing at the origin is the exchange contribution [31], $K^{\mathrm{eff}} = [K^{\mathrm{hom}} + (K^{\mathrm{hom}})^T]/2 = \{\kappa_{ij}\}$ is a symmetric second-rank curvature-induced effective anisotropy tensor with $i, j = 1, 2, 3$, and the homogenized anisotropy matrix K^{hom} takes the form

$$K^{\mathrm{hom}} = \frac{1}{2\pi} \int d\mathbf{y}' \int_{\mathbb{R}^2} d\mathbf{z}' \mathbf{n}(\mathbf{y}') \otimes \mathbf{n}(\mathbf{z}' + \mathbf{y}')[g(0) - g(1)] \tag{4}$$

with

$$g(a) = \frac{1}{\sqrt{|\mathbf{z}'|^2 + |a + f(\mathbf{z}' + \mathbf{y}') - f(\mathbf{y}')|^2}} \tag{5}$$

and $\mathbf{n}(\mathbf{y}') = (-\nabla f(\mathbf{y}'), 1)$. Here the integration over $\mathbf{y}'$ is performed in a unit square $[0, 1] \times [0, 1]$. We note that tensor K^{eff} is non-negative definite, because the last term on the right-hand side of Eq. (3) is derived from the non-negative magnetostatic energy $\int_{\mathbb{R}^3} |\nabla u|^2$.

The main result of this Letter describing the effective anisotropy behavior is based on Eqs. (4) and (5). In the following, we show that in thin films with periodic curvature one can engineer PMA or a uniaxial anisotropy of any particular orientation by choosing the surface shape $f(x_1, x_2)$ appropriately. This can open doors for tailoring materials with a given anisotropy direction.

We first consider simpler, effectively one-dimensional (1D) case, when the 2D structure changes periodically only in one direction (we choose this direction to be $\hat{\mathbf{x}}_1$). In this case, $f(x_1, x_2) = f(x_1)$, and after integrating Eq. (4) over y_2 and z_2, we obtain

$$K_{1D}^{\text{hom}} = \frac{1}{4\pi}\int_0^1 dy_1 \int_{-\infty}^{\infty} dz_1 \mathbf{n}(y_1) \otimes \mathbf{n}(z_1 + y_1) \times \log \frac{z_1^2 + [1 + f(z_1 + y_1) - f(y_1)]^2}{z_1^2 + [f(z_1 + y_1) - f(y_1)]^2}. \quad (6)$$

It is easy to check in Eq. (6) that all effective matrix elements $\kappa_{i2} = \kappa_{2i} = 0$, and therefore zero is guaranteed to be the minimal eigenvalue of K^{eff} with the eigenvector $\hat{\mathbf{x}}_2$. If the zero eigenvalue is not degenerate, $\hat{\mathbf{x}}_2$ is the easy axis of anisotropy. Alternatively, if zero is an eigenvalue of multiplicity two, the anisotropy is of the easy x_1x_2-plane type. For example, this is the case when $f(x_1) = \text{const}$. To conclude, for the structures periodically changing along the x_1 direction, one can obtain only x_1x_2 easy-plane or easy-axis anisotropy along $\hat{\mathbf{x}}_2$.

To explain the main ideas of how to engineer specific anisotropies, we next consider a truly 1D case by disregarding the $\hat{\mathbf{x}}_2$ direction and investigating the anisotropy in the x_1x_3 plane only. In this case, K_{1D}^{eff} is reduced to a 2×2 matrix:

$$K_{1D}^{\text{eff}} = \begin{pmatrix} \kappa_{11} & \kappa_{13} \\ \kappa_{13} & \kappa_{33} \end{pmatrix}, \quad (7)$$

and the anisotropy orientation is determined by its eigenvalues and eigenvectors. If the minimal eigenvalue of K_{1D}^{eff},

$$\lambda_{\min} = (\kappa_{11} + \kappa_{33})/2 - \sqrt{(\kappa_{11} - \kappa_{33})^2/4 + \kappa_{13}^2}, \quad (8)$$

is not degenerate (i.e., $\kappa_{11} \neq \kappa_{33}$ or $\kappa_{13} \neq 0$), its eigenvector direction defines the easy axis of the anisotropy. Alternatively, if it is degenerate, the anisotropy is of the x_1x_3 easy-plane type. For nondegenerate $\lambda_{\min}$, the anisotropy direction lies in the x_1x_3 plane and makes angle ϕ with $\hat{\mathbf{x}}_1$:

$$\phi = \arctan\left(\frac{1}{\gamma}\left[1 - \text{sgn}(\kappa_{33} - \kappa_{11})\sqrt{\gamma^2 + 1}\right]\right) \quad (9)$$

for $\kappa_{11} \neq \kappa_{33}$, where $\gamma = 2\kappa_{13}/(\kappa_{33} - \kappa_{11})$, and in the special case $\kappa_{11} = \kappa_{33}$ and $\kappa_{13} \neq 0$ the angle $\phi = -(\pi/4)\text{sgn}(\kappa_{13})$.

To be more specific, we consider 1D films whose profile is given on each period by a triangle; see Fig. 2(a). Such a profile is completely characterized by the triangle's height H and the position of the top vertex x_*, so on $[0, 1]$ it is given by

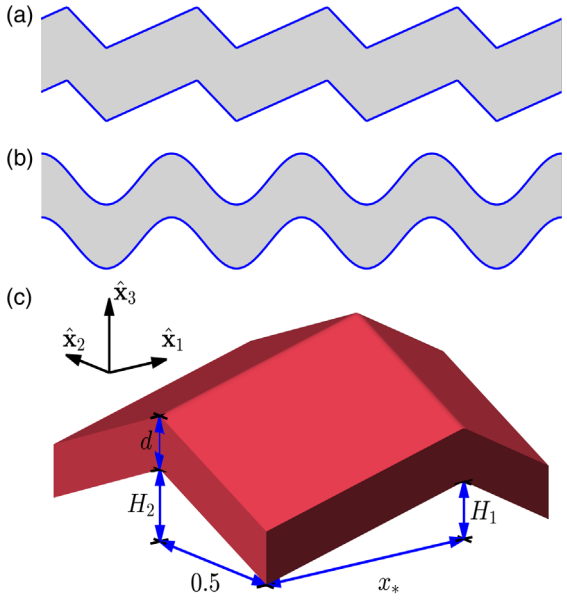

FIG. 2. (a),(b) Cross sections of thin films with periodic (a) pyramid and (b) $\sin^2 x_1 \sin^2 x_2$ textures. (c) One pyramid of the periodic structure shown in Fig. 1(a).

$$f_1(x_1; H, x_*) = \begin{cases} H\frac{x_1}{x_*}, & 0 < x_1 \leq x_*, \\ H\frac{1-x_1}{1-x_*}, & x_* < x_1 \leq 1. \end{cases} \quad (10)$$

One can show analytically that by varying x_* and H it is possible to align the easy-axis anisotropy with any direction in the x_1x_3 plane. Here for simplicity we base our explanation on the results of numerical simulations presented in Fig. 3, where anisotropy angle ϕ as a function of the triangle's height H is calculated for the periodic 1D structure given by Eq. (10). First, we notice that setting $H = 0$ results in the easy axis aligned with $\hat{\mathbf{x}}_1$. Figure 3 shows that increasing the triangle's height H, while holding $x_* > 0.5$ fixed, continuously turns the easy axis from 0 to $\pi/2$. The special case of the symmetric triangles, $x_* = 0.5$, yields the easy-axis anisotropy along $\hat{\mathbf{x}}_1$ ($\phi = 0$) below the critical value of the triangle's height $H_c \simeq 1.8$ and along $\hat{\mathbf{x}}_3$ ($\phi = \pi/2$) above H_c. For $H = H_c$ the anisotropy is of the easy-plane type. Thus, the range $[0, \pi/2]$ for the anisotropy angles can be covered by varying x_* in a reasonable range above 0.5 and H from zero to large enough $H > H_c$. Now by changing parameter x_* from $x_* > 0.5$ presented in Fig. 3 to $x_* < 0.5$, due to the property $\phi(H, 1 - x_*) = -\phi(H, x_*)$, we can rotate the easy-axis anisotropy by $\pi/2$ and cover the range $[-\pi/2, 0]$. As a result, we conclude that in the 1D case one can cover the entire range $[-\pi/2, \pi/2]$ of the easy-axis anisotropy orientations in the x_1x_3 plane.

Next, we study a more general case of 2D structures modulated in both the $\hat{\mathbf{x}}_1$ and $\hat{\mathbf{x}}_2$ directions. Two examples of these periodic structures, made of pyramids and $\sin^2(x_1)\sin^2(x_2)$ functions, are shown in Fig. 1. To be

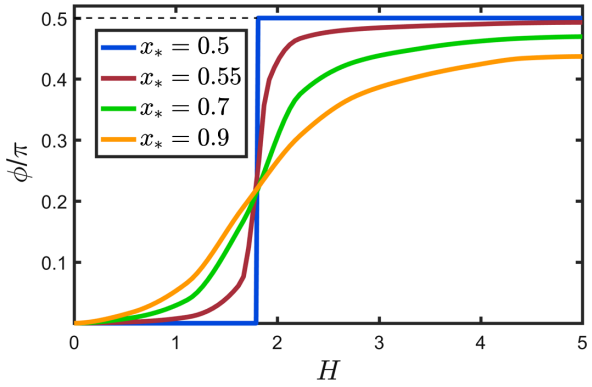

FIG. 3. Angle ϕ the anisotropy makes with $\hat{\mathbf{x}}_1$ as a function of the triangle's height H in the 1D case shown in Fig. 2(a).

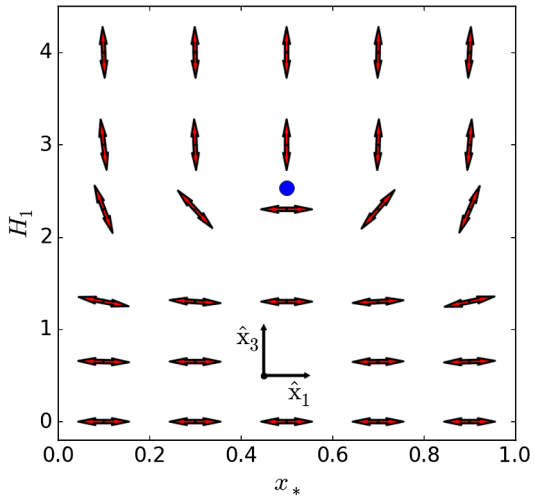

FIG. 4. Direction of anisotropy in the film depicted in Fig. 2(c) as a function of the pyramid's height H_1 and the position of the apex x_* along $\hat{\mathbf{x}}_1$. The film lies in the x_1x_2 plane, and the base of each pyramid is a unit square.

more specific and show the essential physics, we concentrate on a periodic structure made of pyramids depicted in Fig. 2(c). Such a pyramid on a base of a unit square $[0,1]\times[0,1]$ with the apex located at $(x_*, 0.5)$ is modeled by the function

$$f(x_1,x_2;H_1,x_*) = f_1(x_1;H_1,x_*) + f_2(x_2;H_2,0.5), \quad (11)$$

where $f_{1,2}$ are given by Eq. (10). We choose in Eq. (11) the pyramid to be symmetric along x_2, because it will be sufficient to show the essential features by varying the asymmetry only along x_1. Since $f_2(x_2;H_2,0.5)$ is a symmetric function, i.e., $f_2(x_2)=f_2(1-x_2)$, the anisotropy matrix takes the form

$$K^{\text{eff}} = \begin{pmatrix} \kappa_{11} & 0 & \kappa_{13} \\ 0 & \kappa_{22} & 0 \\ \kappa_{13} & 0 & \kappa_{33} \end{pmatrix}, \quad (12)$$

which is easy to show by exploiting the symmetries of Eq. (4). For Eq. (12), $\hat{\mathbf{x}}_2$ is always an eigenvector of K^{eff} with the eigenvalue κ_{22}. Hence, the other eigenvalues and eigenvectors of K^{eff} are determined by analyzing the reduced matrix given by Eq. (7) and have been already described in the 1D case.

To confine the easy axis to the x_1x_3 plane, it is sufficient to choose the parameters so that either of the conditions $\kappa_{11} < \kappa_{22}$ or $\kappa_{33} < \kappa_{22}$ is satisfied. For this, we choose H_2 to be fixed and large enough, while H_1 and x_* are allowed to vary. Then, the anisotropy is of the easy-axis type provided $\kappa_{11} \neq \kappa_{33}$ or $\kappa_{13} \neq 0$. Using similar arguments as in the 1D case, we can show that it is possible to cover the entire range of directions in the x_1x_3 plane. The corresponding results of numerical simulations using the Monte Carlo technique are presented in Fig. 4, which shows the picture qualitatively identical to the 1D problem. We numerically observe that the value $H_2 = 5$ is large enough in the above discussed sense and use it in the simulations. The value of H_c, where for $x_* = 0.5$ the anisotropy orientation abruptly changes from $\hat{\mathbf{x}}_1$ to $\hat{\mathbf{x}}_3$, is found to be $\simeq 2.52$ for $H_2 = 5$; it is shown by the blue point in Fig. 4.

To obtain the preferred anisotropy in any direction, it is enough to rotate the pyramids by an appropriate angle in the x_1x_2 plane and repeat the same arguments as above. Analogous results can be obtained for smooth 2D functions such as $\sin^2(\pi x_1)\sin^2(\pi x_2)$ shown in Fig. 1(b), etc.

Discussion.—The result of this Letter shows that, in spite of the conventional belief [32] that the dipolar interaction in films thicker than a monolayer would put the magnetization in the plane of the film, in the case of particular surface modulation (or periodic roughness) this interaction can lead to perpendicular or any other uniaxial anisotropy. The problem considered above with the same periodic profile on both surfaces can be extended even further. In Supplemental Material, we provide the reduced model for the more general case, where the bottom and top profiles of the film are different [33] (for a rigorous mathematical derivation, see [34]). Moreover, an analogous homogenization technique may be used to treat two coupled magnetic films with periodically modulated surfaces [35,36]; this problem will be treated elsewhere [37].

A possible experimental confirmation of our findings is corroborated by recent efforts to engineer anisotropy in thin films by substrate curvature, following pioneering work [14] and, in particular, Ref. [15], where the PMA has been obtained by depositing in-plane anisotropy Fe-Gd alloys on a nanosphere array. Generally, the magnetic systems studied in Ref. [38] may be excellent candidates for the curvature-induced anisotropy engineering.

The applicability limits of the asymptotic homogenization theory presented here are set by two scales: (i) The lower bound is determined by the validity of the continuous model—i.e., it works on scales larger than interatomic spacing—and (ii) the upper bound is given by the scale of a single domain. Additionally, since the main complexity in

determining the magnetic anisotropy is associated with understanding the influence of the magnetostatic energy, which is nonlocal, without the loss of generality our method can be extended to additively include local terms such as Zeeman energy and crystalline anisotropy.

In summary, we have demonstrated that the PMA can be achieved in thin ferromagnetic films solely due to an interplay of surface curvature and dipolar interactions in the special case of nearly parallel surfaces. This points to the fact that the surface roughness may also significantly modify anisotropy. We have shown how the nonlocal in their nature dipolar interactions, in the presence of an arbitrary large surface curvature of the periodically modulated film, can be reduced to local effective anisotropy term in the micromagnetic energy. We modeled the film surfaces by simple smooth functions $f(x_1, x_2)$, which can, in principle, be engineered in the films, and demonstrated that, by an appropriate choice of $f(x_1, x_2)$, one can orient the magnetic anisotropy axis along any direction. This provides a justification of the concept for future magnetic film nanoengineering with any chosen uniaxial anisotropy without the additional need of heavy-metal layers to provide spin-orbit coupling effects. This method would also allow us to simplify the magnetic structures, by limiting them to only one magnetic layer.

O. A. T. acknowledges support by the Grants-in-Aid for Scientific Research (Grants No. 25247056, No. 15H01009, No. 17K05511, and No. 17H05173) from the Ministry of Education, Culture, Sports, Science and Technology (MEXT) of Japan and MaHoJeRo (DAAD Spintronics network, Project No. 57334897). V. S. and S. V. acknowledge support by the Engineering and Physical Sciences Research Council Grant No. EP/K02390X/1. O. A. T. was supported in part by JSPS and RFBR under the Japan—Russia Research Cooperative Program.

*olegt@imr.tohoku.ac.jp

[1] L. Néel, J. Phys. Radium **15**, 225 (1954).
[2] A. J. Bennett and B. R. Cooper, Phys. Rev. B **3**, 1642 (1971).
[3] H. Takeyama, K. P. Bohnen, and P. Fulde, Phys. Rev. B **14**, 2287 (1976).
[4] M. Kolář, Phys. Status Solidi **96**, 683 (1979).
[5] P. Bruno, J. Appl. Phys. **64**, 3153 (1988).
[6] P. Bruno and J.-P. Renard, Appl. Phys. A **49**, 499 (1989).
[7] R. Arias and D. L. Mills, Phys. Rev. B **59**, 11871 (1999).
[8] G. H. O. Daalderop, P. J. Kelly, and M. F. H. Schuurmans, Phys. Rev. B **42**, 7270 (1990).
[9] P. Bruno, Phys. Rev. B **39**, 865 (1989).
[10] K. Kyuno, R. Yamamoto, and S. Asano, J. Phys. Soc. Jpn. **61**, 2099 (1992).
[11] D. S. Wang, R. Wu, and A. J. Freeman, Phys. Rev. Lett. **70**, 869 (1993).
[12] D. S. Wang, R. Wu, and A. J. Freeman, Phys. Rev. B **48**, 15886 (1993).
[13] S. Peng, M. Wang, H. Yang, L. Zeng, J. Nan, J. Zhou, Y. Zhang, A. Hallal, M. Chshiev, K. L. Wang, Q. Zhang, and W. Zhao, Sci. Rep. **5**, 18173 (2016).
[14] M. Albrecht, G. Hu, I. L. Guhr, T. C. Ulbrich, J. Boneberg, P. Leiderer, and G. Schatz, Nat. Mater. **4**, 203 (2005).
[15] E. Amaladass, B. Ludescher, G. Schütz, T. Tyliszczak, M.-S. Lee, and T. Eimüller, J. Appl. Phys. **107**, 053911 (2010).
[16] G. Carbou, Math. Models Methods Appl. Sci. **11**, 1529 (2001).
[17] V. Slastikov, Math. Models Methods Appl. Sci. **15**, 1469 (2005).
[18] K. Chen, R. Frömter, S. Rössler, N. Mikuszeit, and H. P. Oepen, Phys. Rev. B **86**, 064432 (2012).
[19] Y. Gaididei, V. P. Kravchuk, and D. D. Sheka, Phys. Rev. Lett. **112**, 257203 (2014).
[20] A. Goussev, J. M. Robbins, V. Slastikov, and O. A. Tretiakov, Phys. Rev. B **93**, 054418 (2016).
[21] Y. Gaididei, A. Goussev, V. P. Kravchuk, O. V. Pylypovskyi, J. Robbins, D. D. Sheka, V. Slastikov, and S. Vasylkevych, Journal of Physics A, DOI: 10.1088/1751-8121/aa8179 (2017).
[22] C. Chappert and P. Bruno, J. Appl. Phys. **64**, 5736 (1988).
[23] R. Streubel, J. Lee, D. Makarov, M.-Y. Im, D. Karnaushenko, L. Han, R. Schäfer, P. Fischer, S.-K. Kim, and O. Schmidt, Adv. Mater. **26**, 316 (2014).
[24] D. Makarov, M. Melzer, D. Karnaushenko, and O. G. Schmidt, Appl. Phys. Rev. **3**, 011101 (2016).
[25] A. Bedoya-Pinto, M. Donolato, M. Gobbi, L. E. Hueso, and P. Vavassori, Appl. Phys. Lett. **104**, 062412 (2014).
[26] O. Lee, L. You, J. Jang, V. Subramanian, and S. Salahuddin, Appl. Phys. Lett. **107**, 252401 (2015).
[27] R. Streubel, P. Fischer, F. Kronast, V. P. Kravchuk, D. D. Sheka, Y. Gaididei, O. G. Schmidt, and D. Makarov, J. Phys. D **49**, 363001 (2016).
[28] See Supplemental Material at http://link.aps.org/supplemental/10.1103/PhysRevLett.119.077203 for details.
[29] G. Allaire, SIAM J. Math. Anal. **23**, 1482 (1992).
[30] G. Dal Maso, *An Introduction to* Γ*-Convergence* (Birkhäuser, Boston, 1993).
[31] See Supplemental Material at http://link.aps.org/supplemental/10.1103/PhysRevLett.119.077203 for the exact analytical expression.
[32] J. G. Gay and R. Richter, Phys. Rev. Lett. **56**, 2728 (1986).
[33] See Supplemental Material at http://link.aps.org/supplemental/10.1103/PhysRevLett.119.077203 for the expression and more details.
[34] M. Morini and V. Slastikov, arXiv:1705.01742.
[35] L. Néel, C. R. Acad. Sci. **255**, 1676 (1962).
[36] B. D. Schrag, A. Anguelouch, S. Ingvarsson, G. Xiao, Y. Lu, P. L. Trouilloud, A. Gupta, R. A. Wanner, W. J. Gallagher, P. M. Rice, and S. S. P. Parkin, Appl. Phys. Lett. **77**, 2373 (2000).
[37] M. Morini, V. Slastikov, and O. A. Tretiakov (unpublished).
[38] D. K. Ball, K. Lenz, M. Fritzsche, G. Varvaro, S. Günther, P. Krone, D. Makarov, A. Múcklich, S. Facsko, J. Fassbender, and M. Albrecht, Nanotechnology **25**, 085703 (2014).